IrPd, IrHg, IrCu, and IrTl Binuclear Complexes Bridged by the Short-Bite Ligand 2-(Diphenylphosphino)pyridine. Catalytic Effect in the Hydroformylation of Styrene Due to the Monodentate P-Bonded 2-(Diphenylphosphino)pyridine Ligands of *trans*-[Ir(CO)(Ph_2PPy)$_2$Cl]

Giancarlo Franciò, Rosario Scopelliti, Carmela Grazia Arena, Giuseppe Bruno, Dario Drommi, and Felice Faraone*

Dipartimento di Chimica Inorganica, Chimica Analitica e Chimica Fisica dell'Università, Salita Sperone 31, Villaggio S. Agata, I-98166 Messina, Italy

Received February 25, 1997

The complex *trans*-[Ir(CO)Cl(Ph_2PPy)$_2$] (**1**; Ph_2PPy = 2-(diphenylphosphino)pyridine) was obtained in good yield from the reaction of [Ir(*p*-toluidine)$(CO)_2$Cl] with Ph_2PPy. It has a square-planar geometry, as does the analogous Vaska complex, with two monodentate Ph_2PPy ligands P-bonded to the iridium(I) center. Compound **1** exhibits a reactivity reminiscent of Vaska's complex; in fact, it adds SO_2, halogens, HCl, and CH_3I. The addition of HCl to **1** initially occurs at the pyridine nitrogen atoms of the pendant Ph_2PPy and subsequently at the iridium(I) center, affording [Ir(CO)H$(Cl)_2$(Ph_2PPyH)$_2$][Cl]$_2$ (**6**). The addition of a benzene solution of [Pd$(PhCN)_2Cl_2$] to a solution of **1** in the same solvent yielded, nearly quantitatively, the $Ir^{II}Pd^{I}$ complex [IrPd(CO)Cl_3(μ-Ph_2PPy)$_2$] (**8**). The reaction of **1** with $HgCl_2$, in benzene, in a 1:1 molar ratio afforded the binuclear complex [Ir(CO)Cl_2(μ-Ph_2PPy)$_2$HgCl] (**9**). Using a 1:2 molar ratio the product [Ir(CO)Cl_2($HgCl_2$)(μ-Ph_2PPy)$_2$HgCl]·2CH_2Cl_2 (**10**) was obtained. Compounds **8** and **10** were also characterized by a single-crystal X-ray diffraction analysis. The reaction of **1** with [Cu$(NCCH_3)_4$]BF_4 afforded, almost quantitatively, the ionic compound [Ir(CO)Cl(μ-Ph_2PPy)$_2$Cu]BF_4 (**11**) as an orange solid. The compound [Ir(CO)Cl(μ-Ph_2PPy)$_2$Tl]-PF_6 (**12**) obtained from the reaction of **1** with $TlPF_6$, shows the Ir−Tl bonding and is luminescent in frozen CH_2Cl_2 solution at 77 K with a lifetime of 5 ns (±10%). As opposed to analogous compounds, in the bimetallic complexes **8**−**12** the bridging Ph_2PPy ligands assume a head-to-head structure. The aim of the work was to obtain some insight into the beneficial effect of catalytic precursors containing the pendant Ph_2PPy ligand in the hydroformylation catalytic cycle. Using complex **1** as a precatalyst in the hydroformylation of styrene, at 80 °C and under 80 atm of CO/H_2 (1:1) pressure, the rate of the catalytic process increases significantly with respect to that observed with Vaska's complex, making clear a favorable effect of the pendant Ph_2PPy ligand. However, the chemoselectivity of the process was low. A scheme of the catalytic cycle is proposed. The new aspects of the catalytic cycle are: (i) the protonation under equilibrium conditions of one of the two pyridine nitrogen atoms of the pendant Ph_2PPy ligands in the reductive elimination of HCl from the dihydride−iridium(III) species formed by oxidative addition of H_2 to **1** and (ii) protonolysis, by the proton coordinated to the pyridine nitrogen atom, of the acyl or σ-alkyl groups present in the intermediates formed in the reaction pathway. Unexpectedly, **11** and **12** exhibit catalytic activity comparable with that of **1**. This occurs because under the experimental conditions used the Cu−N or Tl−N bonds are broken, giving **1**.

Introduction

Recently[1] some of us studied the catalytic hydroformylation system obtained *in situ* by addition of 2-(diphenylphosphino)pyridine (Ph_2PPy) to [RhH(CO)-$(PPh_3)_3$], at variable ligand-to-metal ratios. At first it was shown by $^{31}P\{^1H\}$ NMR that in solution Ph_2PPy easily displaces 1 or 2 mol of PPh_3 from Wilkinson's catalyst, giving rise to mixed mononuclear rhodium(I) complexes. These species, namely [RhH(CO)$(PPh_3)_2$(Ph_2-PPy)] and [RhH(CO)(PPh_3)($Ph_2PPy)_2$], contain the Ph_2PPy as a monodentate P-bonded ligand and show a structure similar to that of [RhH(CO)$(PPh_3)_3$]. The results demonstrate that the addition of Ph_2PPy to Wilkinson's catalyst exerted a beneficial effect on the rhodium-catalyzed hydroformylation of styrene as an improvement in the rate of the low-pressure catalytic reaction was observed. This favorable effect of Ph_2PPy

(1) Gladiali, S.; Pinna, L.; Arena, C. G.; Rotondo, E.; Faraone, F. *J. Mol. Catal.* **1991**, *66*, 183.

S0276-7333(97)00145-3 CCC: $15.00
Publication on Web 01/07/1998

was considered to be due to the presence of basic nitrogen in the pendant pyridine.

Subsequently, new catalytic systems, formed by the combination of a ligand containing the 2-(diphenylphosphino)pyridine moiety with a palladium(II) species and an acid of weakly coordinating anions, have been developed for the carbonylation of alkynes.[2] Such catalytic systems have been applied in the selective production of methyl methacrylate by methoxycarbonylation of propyne and in the synthesis of Naproxen precursors.[3] The catalytic activity was considered to be due to the presence of monodentate P-bonded Ph_2PPy, which can be protonated and acts as an effective "proton messenger".

Here we report on the results obtained in the hydroformylation of styrene using as precatalyst the complex *trans*-[Ir(CO)(Ph_2PPy)$_2$Cl] (**1**) structurally analogous to Vaska's complex. The choice of **1** as catalyst precursor has been effected because, in the tertiary phosphine complexes *trans*-[Ir(CO)(PR_3)$_2$Cl], the iridium(I) center is so basic that substrate activation affords very stable iridium(III) species which are not able to promote the catalytic cycle.[4] Thus, the catalytic activity observed using **1** as catalyst precursor can be due to the presence of the uncoordinated nitrogen atom in the pendant Ph_2PPy ligands.

In addition, owing to the lack of reports[5] on the chemistry of iridium(I) species containing the bifunctional ligand Ph_2PPy, we synthesized Ir−Cu, Ir−Tl, Ir−Hg, and Ir−Pd bimetallic species containing bridged Ph_2PPy ligands. The solid-state structures of [Ir(CO)Cl_2($HgCl_2$)(μ-Ph_2PPy)$_2$HgCl] and [Ir(CO)Cl_2(μ-Ph_2PPy)$_2$PdCl] were determined by X-ray diffraction and are reported herein. The cationic species [Ir(CO)Cl(μ-Ph_2PPy)$_2$Cu]BF_4 (**11**) and [Ir(CO)Cl(μ-Ph_2PPy)$_2$Tl]PF_6 (**12**) were also employed as catalytic precursors in the hydroformylation of styrene. These catalytic bimetallic systems were chosen in an attempt to afford insight into the action of the cocatalyst, generally a metal salt, in some catalytic cycles. For example,[6] a patent reported that 1-butene can be produced from ethylene with 90% selectivity, using as the catalytic system $Pd(OAc)_2$, Ph_2PPy, and cupric trifluoromethanesulfonate, in diglyme.

Experimental Section

Established methods were used to prepare the compounds [Ir(CO)$_2$(*p*-toluidine)Cl],[7] [Cu(NCMe)$_4$]BF_4,[8] [Pd(PhCN)$_2$Cl$_2$],[9] and Ph_2PPy.[5] All other reagents were purchased and used as supplied.

Solvents were dried by standard procedures. All experiments were performed under an atmosphere of purified nitrogen. IR spectra were obtained as Nujol mulls on KBr or CsI plates using a Perkin-Elmer FTIR 1720 spectrophotometer. Absorption spectra in the UV and visible regions were performed with a Kontron Uvikon 860 spectrophotometer. Luminescence spectra were recorded with a Perkin-Elmer LS-5B spectrofluorimeter equipped with a red-sensitive Hamamatsu R928 phototube, and luminescence lifetimes were measured with an Edinburgh FL 900 single-photon-counting spectrometer. For the low-temperature measurements, a homemade finger Dewar was employed. ^{1}H and ^{31}P{^{1}H} NMR spectra were recorded on a Bruker AMX R300. ^{1}H NMR spectra were referenced to internal tetramethylsilane and ^{31}P{^{1}H} spectra to external 85% H_3PO_4; positive chemical shifts are for all nuclei to higher frequency. Gas chromatographic analyses were run on a Carlo Erba HRGC 5160 Mega Series apparatus (split/splitless injector, MEGA OV1 25 m column, film thickness 2 μm, carrier gas He, FID detector). Elemental analyses were performed by Redox s.n.c., Cologno Monzese, Milano, Italy.

Syntheses. *trans*-[Ir(CO)(Ph_2PPy)$_2$Cl] (1). A benzene solution (30 mL) of Ph_2PPy (0.404 g, 1.535 mmol) was added to a stirred solution of [Ir(CO)$_2$(*p*-toluidine)Cl] (0.300 g, 0.767 mmol) in the same solvent (50 mL). During the addition, the mixture turned yellow. After 1 h, the solvent was removed at reduced pressure and the yellow solid was washed with petroleum ether (bp 40−60 °C) and dried *in vacuo*. Yield: 95% (0.570 mg, 0.729 mmol). Anal. Calcd for $C_{35}H_{28}ClP_2N_2OIr$: C, 53.74; H, 3.61; N, 3.58; Cl, 4.53. Found: C, 53.80; H, 3.66; N,3.52; Cl, 4.50. IR (CsI, Nujol): ν(CO) 1952 cm^{-1}. ^{1}H NMR ($CDCl_3$): δ 8.77 (d, 6-H Py). ^{31}P{^{1}H} NMR ($CDCl_3$): δ 24.46 (s).

Reaction of 1 with SO_2. Sulfur dioxide was slowly bubbled through a benzene solution (10 mL) of **1** (0.110 g, 0.141 mmol) for about 5 min. During this time the solution color turned from yellow to pale green. Then hexane (30 mL) was added to give a pale green solid. This was separated by filtration and washed with diethyl ether and dried in vacuo. The pure product [Ir(CO)(Ph_2PPy)$_2$(SO_2)Cl] (**2**) was obtained in 95% yield (0.113 g, 0.134 mmol). Anal. Calcd for $C_{35}H_{28}ClP_2N_2O_3SIr$: C, 49.67; H, 3.33; N, 3.31; Cl, 4.19; S, 3.79. Found: C, 49.72; H, 3.31; N, 3.01; Cl, 3.99; S, 3.25. IR (CsI, Nujol): ν(CO) 2023 cm^{-1}, ν(SO) 1143, 1055 cm^{-1}. ^{1}H NMR ($CDCl_3$): δ 8.77 (d, 6-H Py). ^{31}P{^{1}H} NMR ($CDCl_3$): δ 14.69 (s).

[Ir(CO)(Ph_2PPy)$_2$(Br_2)Cl] (3). To a dichloromethane solution (20 mL) of **1** (0.090 g, 0.115 mmol) was added a solution of bromine in the same solvent dropwise until the IR spectrum indicated the disappearance of the ν(CO) band of the starting material. After $^1/_2$ h, the volume of the mixture was reduced to ca. 10 mL. By addition of hexane (30 mL) an orange precipitate was obtained. This was filtered, washed with diethyl ether, and dried in vacuo to give **3** in 75% yield (0.081 g, 0.086 mmol). Anal. Calcd for $C_{35}H_{28}Br_2ClP_2N_2OIr$: C, 44.62; H, 3.00; N, 2.97; Cl, 3.76; Br, 16.96. Found: C, 44.72; H, 3.11; N, 3.01; Cl, 3.99; Br, 17.15. IR (CsI, Nujol): ν(CO) 2040 cm^{-1}. ^{1}H NMR ($CDCl_3$): δ 8.81 (d, 6-H Py, 2H). ^{31}P{^{1}H} NMR ($CDCl_3$): δ 18.10 (s).

[Ir(CO)(Ph_2PPy)$_2$Cl(I_2)] (4). This compound was obtained similarly to **3**, as a brown-orange solid in 70% yield, by adding I_2 to a CH_2Cl_2 solution of **1**. Anal. Calcd for $C_{35}H_{28}I_2ClP_2N_2OIr$: C, 40.58; H, 2.72; N, 2.70; Cl, 3.42; I, 24.50. Found: C, 40.53; H, 2.68; N, 2.65; Cl, 3.38; I, 24.75. IR (CsI, Nujol): ν(CO) 2042 cm^{-1}. ^{1}H NMR ($CDCl_3$): δ 8.78 (d, 6-H Py). ^{31}P{^{1}H} NMR ($CDCl_3$): δ 17.80 (s).

[Ir(CO)(Ph_2PPy)$_2$(H_2)Cl] (5). Hydrogen was slowly bubbled through a dichloromethane solution (20 mL) of **1** (0.080 g, 0.102 mmol) for about 2 h. During this time, the yellow color disappeared. Then the solvent was removed, under an atmosphere of hydrogen, and the white solid **5** obtained was washed with diethyl ether. Yield: 95% (0.76 g, 0.97 mmol). Anal. Calcd for $C_{35}H_{30}ClP_2N_2OIr$: C, 53.70; H, 3.86; N, 3.57; Cl, 4.52. Found: C, 53.82; H, 3.96; N, 3.52; Cl, 4.44. IR (CsI, Nujol): ν(CO) 1984, ν(MH) 2194, 2104 cm^{-1}. ^{1}H NMR ($CDCl_3$): δ 8.77

(2) Drent, E.; Arnoldy, P.; Budzelaar, P. H. M. *J. Organomet. Chem.* **1993**, *455*, 247; **1994**, *475*, 57.
(3) Scrivanti, A.; Matteoli, U. *Tetrahedron Lett.* **1995**, 9015.
(4) (a) Crabtree, R. H. *The Organometallic Chemistry of the Transition Metals;* Wiley: New York, 1988; p 192. (b) Henrici-Olivé, G.; Olivé, S. *Coordination and Catalysis*; Verlag Chemie: Weinheim, Germany, 1976; pp 162, 236. (c) Halpern, J. *Acc. Chem. Res.* **1970**, *3*, 386.
(5) Newkome, G. R. *Chem. Rev.* **1993**, *93*, 2067.
(6) Drent, E. Eur. Pat. Appl. EP 307,026, 1989.
(7) Kablunde, V. *Inorg. Synth.* **1974**, *15*, 82.
(8) Kubas, G. J. *Inorg. Synth.* **1979**, *19*, 90.
(9) Doyle, J.; Slade, P. E.; Jonassen, H. B. *Inorg. Synth.* **1960**, 6, 218.

Table 1. Crystal Data and Structure Determination Summary for 8 and 10

	8	10
formula	$C_{35}H_{28}Cl_3IrN_2OP_2Pd\cdot H_2O$	$C_{35}H_{28}Cl_5Hg_2IrN_2OP_2\cdot 2CH_2Cl_2$
M_r	975.48	1495.02
temp (K)	293(2)	293(2)
cryst syst	orthorombic	triclinic
space group	$P2_12_12_1$	$P\bar{1}$
a (Å)	10.361(2)	10.094(2)
b (Å)	15.894(2)	12.773(3)
c (Å)	21.711(5)	20.198(4)
α (deg)	90	72.22(2)
β (deg)	90	78.16(2)
γ (deg)	90	69.67(2)
V (Å^3)	3575(1)	2310.9(8)
Z	4	2
F(000)	1888	1392
D_{calcd} (g cm^{-3})	1.812	2.149
λ(Mo Kα) (Å)	0.710 73	0.710 73
μ (Mo Kα) mm^{-1}	4.569	10.121
θ range (deg)	1.5−27.5	1.5−27
index ranges	$0 \le h \le 14$, $0 \le k \le 21$, $0 \le l \le 29$	$0 \le h \le 13$, $-17 \le k \le 17$, $-26 \le l \le 26$
no. of rflns collected	4749	10 891
no. of unique rflns	4603	10 134
no. of refined params	415	488
GOF on F^2	0.931	0.843
$R1$ (on F, $I > 2\sigma(I)$)	0.0412	0.0795
wR2 (on F^2, all data)	0.1037	0.2912

(d, 6-H Py), −7.54 (td, IrH, 1H, J_{PH} 17.7 Hz, J_{HH} 4.8 Hz), −18.68 (td, IrH, 1H, J_{PH} 14.3 Hz, J_{HH} 4.8 Hz). $^{31}P\{^1H\}$ NMR ($CDCl_3$): δ 11.85 (s).

[Ir(CO)(H)(Ph$_2$PPyH)$_2$(Cl)$_2$][Cl]$_2$ (6). To a dichloromethane solution (30 mL) of **1** (0.150 g, 0.192 mmol) was added a 1 M aqueous solution of HCl (0.576 mL). After 1 h, the resultant pale yellow solution was reduced to ca. 10 mL. By addition of diethyl ether (40 mL) a pale yellow precipitate was obtained. This was filtered, washed with diethyl ether, and dried in vacuo to give **6** in 80% yield (0.137 g, 0.153 mmol). Anal. Calcd for $C_{35}H_{31}Cl_4P_2N_2OIr$: C, 47.15; H, 3.50; N, 3.14; Cl, 15.90. Found: C, 47.20; H, 3.55; N, 3.08; Cl, 15.65. IR (CsI, Nujol): ν(CO) 2040 cm^{-1}. ^1H NMR ($CDCl_3$): δ 8.75 (d, 6-H Py), −15.49 (t, IrH, 1H, J_{PH} 11.88 Hz). $^{31}P\{^1H\}$ NMR ($CDCl_3$): δ 0.76 (s).

[Ir(CO)(CH$_3$)ClI(Ph$_2$PPy)$_2$] (7). A solution of **1** (0.087 g, 0.111 mmol) dissolved in iodomethane (1.5 mL) was stirred for 10 min. Then the excess of CH_3I was evaporated under reduced pressure to give **7** as a yellow solid. It was washed with diethyl ether (40 mL) and dried. Yield: 90% (0.092 g, 0.100 mmol). Anal. Calcd for $C_{36}H_{31}ClP_2N_2IOIr$: C, 46.79; H, 3.38; N, 3.03; Cl, 3.84. Found: C, 46.85; H, 3.45; N, 3.12; Cl, 3.70. IR (CsI, Nujol): ν(CO) 2045 cm^{-1}. ^1H NMR ($CDCl_3$): δ 8.77 (d, 6-H Py), 0.90 (t, CH_3, 3H, J_{PH} 5.4 Hz). $^{31}P\{^1H\}$ NMR ($CDCl_3$): δ 17.20 (s).

[Ir(CO)(Cl)$_2$(μ-Ph$_2$PPy)$_2$PdCl] (8). To a benzene solution (20 mL) of **1** (0.104 g, 0.133 mmol) was added [Pd(PhCN)$_2$-(Cl)$_2$] (0.051 g, 0.133 mmol) in the same solvent. During the addition the solution turned red-orange. After 2 h, the solvent was removed by vacuum evaporator and the orange solid was recrystallized from CH_2Cl_2−hexane (1:3) to give the product. Yield: 85% (0.108 g, 0.113 mmol). Anal. Calcd for $C_{35}H_{28}$-$Cl_3P_2N_2OIrPd$: C, 43.81; H, 2.94; N, 2.91; Cl, 11.08. Found: C, 43.35; H, 3.07; N, 3.00; Cl, 10.60. IR (CsI, Nujol): ν(CO) 2016 cm^{-1}. ^1H NMR ($CDCl_3$): δ 9.31 (d, 6-H Py). $^{31}P\{^1H\}$ NMR ($CDCl_3$): δ −12.80 (s).

[Ir(CO)(Cl)$_2$(μ-Ph$_2$PPy)$_2$HgCl] (9). To a stirred solution (25 mL) of **1** (0.100 g, 0.128 mmol) in benzene (25 mL) was added solid $HgCl_2$ (0.035 g, 0.128 mmol). After 3 h, the volume of the solution was reduced to ca. 5 mL *in vacuo*. A white solid was formed by addition of hexane (30 mL). This was separated by filtration, recrystallized from CH_2Cl_2/hexane, and dried. Yield 80% (0.108 g, 0.102 mmol). Anal. Calcd for $C_{35}H_{28}Cl_3P_2N_2OIrHg$: C, 39.89; H, 2.68; N, 2.66; Cl, 10.09. Found: C, 39.80; H, 2.63; N, 2.72; Cl, 10.25. IR (CsI, Nujol): ν(CO) 2026 cm^{-1}. ^1H NMR ($CDCl_3$): δ 9.27 (d, 6-H Py). $^{31}P\{^1H\}$ NMR ($CDCl_3$): δ 16.83 (s).

[Ir(CO)(Cl)$_2$(HgCl$_2$)(μ-Ph$_2$PPy)$_2$HgCl]·2CH$_2$Cl$_2$ (10). To a stirred solution (25 mL) of **1** (0.110 g, 0.141 mmol) in benzene (25 mL) was added solid $HgCl_2$ (0.076 g, 0.282 mmol). After 3 h, the volume of the solution was reduced to ca. 5 mL in vacuo; by addition of hexane (30 mL) a white solid was formed. This was separated by filtration, recrystallized from CH_2Cl_2/hexane, and dried. Yield: 80% (0.190 g, 0.113 mmol). Anal. Calcd for $C_{37}H_{32}Cl_9P_2N_2OIrHg_2$: C, 26.34; H, 1.91; N, 1.66; Cl, 18.91. Found: C, 26.38; H, 1.98; N, 1.72; Cl, 18.99. IR (CsI, Nujol): ν(CO) 2026 cm^{-1}. ^1H NMR ($CDCl_3$): δ 9.27 (d, 6-H Py). $^{31}P\{^1H\}$ NMR ($CDCl_3$): δ 16.83 (s).

[Ir(CO)(Cl)(μ-Ph$_2$PPy)$_2$Cu][BF$_4$] (11). To a stirred solution (25 mL) of **1** (0.110 g, 0.141 mmol) in benzene (25 mL) was added solid [Cu(CH$_3$CN)$_4$][BF$_4$] (0.044 g, 0.141 mmol). After 3 h, the orange solution was vacuum-reduced to ca. 5 mL. An orange solid was obtained by addition of hexane (30 mL). This was separated by filtration, washed with diethyl ether, and dried. Yield: 85% (0.112 g, 0.120 mmol). Anal. Calcd for $C_{35}H_{28}ClP_2N_2OIrCuBF_4$: C, 45.08; H, 3.03; N, 3.00; Cl, 3.80. Found: C, 44.81; H, 3.55; N,3.20; Cl, 3.60. IR (CsI, Nujol): ν(CO) 1983 cm^{-1}, ν(BF$_4$) 1090 cm^{-1}. ^1H NMR ($CDCl_3$): δ 9.39 (d, 6-H Py). $^{31}P\{^1H\}$ NMR ($CDCl_3$): δ 27.44 (s).

[Ir(CO)(Cl)(μ-Ph$_2$PPy)$_2$Tl][PF$_6$] (12). This compound was obtained similarly to **11**, as a red solid, by starting from **1** (0.110 g, 0.141 mmol) and $TlPF_6$ (0.493 g, 0.141 mmol). Yield: 95% (0.151 g, 0.134 mmol). Anal. Calcd for $C_{35}H_{28}ClP_3N_2F_6OIrTl$: C, 37.15; H, 2.49; N, 2.48; Cl, 3.13. Found: C, 38.02; H, 2.80; N, 2.62; Cl, 3.03. IR (CsI, Nujol): ν(CO) 1994 cm^{-1}, ν(PF$_6$) 998 cm^{-1}. ^1H NMR ($CDCl_3$) δ 9.15 (d, 6-H Py). $^{31}P\{^1H\}$ NMR ($CDCl_3$): δ 23.20 (s).

X-ray Data Collection and Structure Refinement of [Ir(CO)(Cl)$_2$(μ-Ph$_2$PPy)$_2$PdCl] (8) and [Ir(CO)(Cl)$_2$(HgCl$_2$)-(μ-Ph$_2$PPy)$_2$HgCl]·2CH$_2$Cl$_2$ (10). Suitable crystals of the complexes **8** and **10** have been obtained by slow evaporation of CH_2Cl_2−hexane solutions. X-ray measurements were made on a Siemens R3m/V four-circle diffractometer. Data were collected at room temperature. A summary of the crystallographic data and the structure refinements is listed in Table 1. No correction for absorption was applied for Ir−Hg because of rapid decay of the crystal under X-ray exposure (about 40%), and this prevented the accuracy of data, as can be seen in

Scheme 1[a]

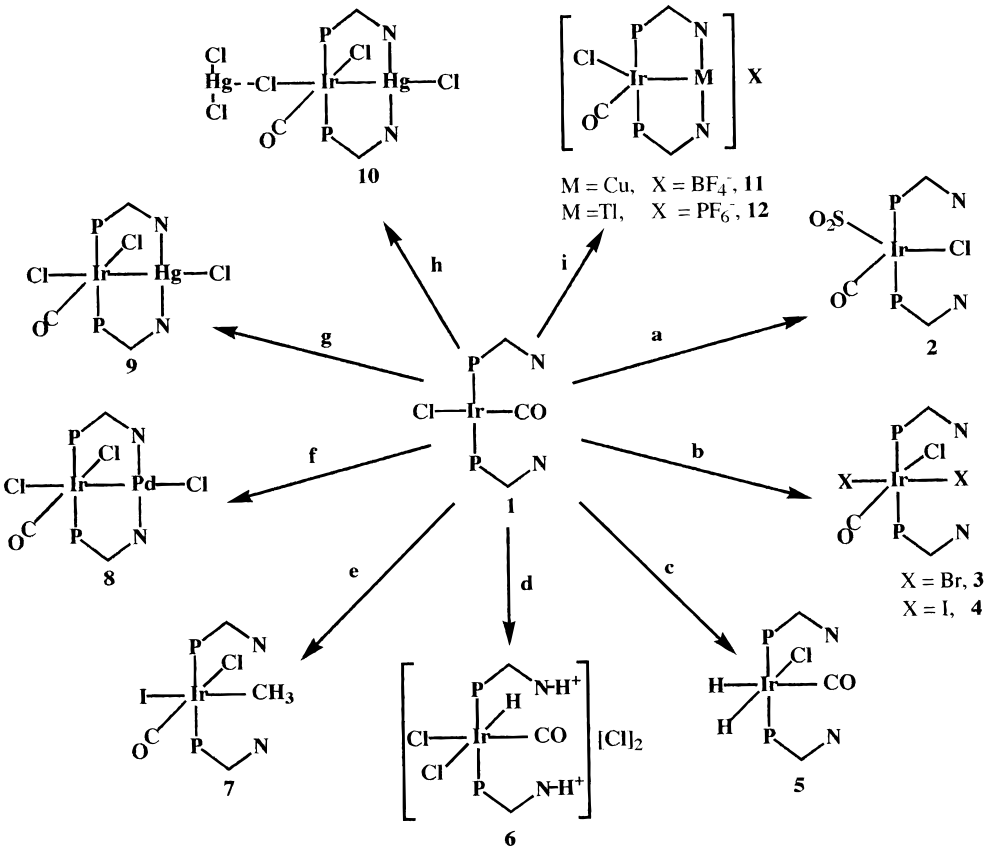

[a] Legend: P−N = 2-(diphenylphosphino)pyridine; (a) SO_2 gas, benzene; (b) Br_2 or I_2, CH_2Cl_2; (c) H_2, CH_2Cl_2; (d) HCl solution, CH_2Cl_2; (e) CH_3I, neat; (f) $[Pd(PhCN)_2Cl_2]$, 1:1 molar ratio, benzene; (g) $HgCl_2$, 1:1 molar ratio, benzene; (h) $HgCl_2$, 1:2 molar ratio, benzene; (i) $[Cu(CH_3CN)_4]BF_4$, 1:1 molar ratio, benzene; $TlPF_6$, 1:1 molar ratio, benzene.

Table 1. Absorption correction for Ir−Pd: minimum and maximum transmissions are 0.746 and 0.792, respectively.

Structures were solved by Patterson and Fourier methods.[10] The refinements were carried out by full-matrix least-squares on F^2 with anisotropic thermal parameters for all non-hydrogen atoms. Hydrogens were placed at their geometrically calculated positions and refined "riding" on the corresponding carbon atoms, with a fixed and unique isotropic displacement parameter (U_{iso} = 0.08 Å^2 for Ir−Hg and 0.07 Å^2 for Ir−Pd). The Flack[11] absolute structure parameter (0.01(1)) confirms for Ir−Hg its correctness. All calculations were performed on a Micro-VAX 3400 and on a DEC Alpha 3000/400 using the SHELXTL 5.0[10] program library. All other data (fractional, etc.) are included in the Supporting Information.

Catalytic Runs. All catalytic runs were performed in a 100 mL Berghoff stainless-steel autoclave equipped with gas and liquid inlets, a heating device, and magnetic stirring. The reactions were carried out in a Teflon vessel fitted to the internal wall of the autoclave, thus preventing undesirable effects due to the metal of the reactor. The autoclave was closed and degassed through three vacuum−nitrogen cycles. A solution of the starting complex and of the olefin (in a typical experiment 5 mmol of substrate and 0.01 mmol of complex), in benzene (10 mL), was introduced under nitrogen, and gases (H_2/CO 1:1) were admitted up to the desired pressure. At the end of each catalytic run, the autoclave was cooled in a cold water bath and slowly vented. A sample of the homogeneous reaction mixture was then analyzed by gas chromatography.

(10) Siemens Energy and Automation Inc., Analytical Instrumentation, Madison, WI, 1996.

(11) Bernardinelli, G.; Flack, H. D. *Acta Crystallogr.* **1985**, *A41*, 500−511.

Results

The reactions described are summarized in Scheme 1.

Synthesis and Reactions of *trans*-[Ir(CO)(Ph$_2$PPy)$_2$Cl] (1). The reaction of [Ir(*p*-toluidine)(CO)$_2$Cl] with Ph_2PPy in a 2:1 ligand to metal ratio, in benzene at room temperature, gave in good yield the new complex *trans*-[Ir(CO)(Ph_2PPy)$_2$Cl] (**1**), which was isolated as a yellow solid soluble in benzene (although nonconducting), chlorinated solvents, and acetone. In solution **1** is not air-stable due to easy uptake of oxygen to give the corresponding adduct. Spectroscopic data support a square-planar geometry for **1** with the two bifunctional ligands Ph_2PPy acting as monodentate P-bonded ligands. In accordance, the IR spectrum of a Nujol mull shows ν(CO) at 1952 cm^{-1} and the $^{31}P\{^1H\}$ NMR spectrum in $CDCl_3$ solution shows a singlet at δ 24.46 ppm. Significantly, the ^1H NMR spectrum, in $CDCl_3$ solution, shows a distinct resonance at δ 8.77 ppm for the 6-hydrogen of the pyridine ring, as usual when the Ph_2PPy acts as a monodentate P-bonded ligand.[12] This resonance is further shifted to higher frequency when the Ph_2PPy acts as a bifunctional ligand. Both $^{31}P\{^1H\}$ and ^1H NMR spectra are temper-

(12) (a) Arena, C. G.; Rotondo, E.; Faraone, F.; Lanfranchi, M.; Tiripicchio, A. *Organometallics* **1991**, *10*, 3877. (b) Arena, C. G.; Bruno, G.; De Munno, G.; Rotondo, E.; Drommi, D.; Faraone, F. *Inorg. Chem.* **1993**, *32*, 1601. (c) Arena, C. G.; Drommi, D.; Faraone, F.; Lanfranchi, M.; Nicolò, F.; Tiripicchio, A. *Organometallics* **1996**, *15*, 3170. (d) Drommi, D.; Arena, C. G.; Nicolò, F.; Bruno, G.; Faraone, F. *J. Organomet. Chem.* **1995**, *485*, 115.

ature-independent, indicating the lack of a fluxional process with formation of five-coordinated species by coordination of the pyridine nitrogen atom of Ph_2PPy ligand to the metal center on the NMR time scale.

Compound **1** exhibits a reactivity similar to that of *trans*-$[Ir(CO)(PPh_3)_2Cl]$;[13,14] in fact, it adds SO_2, halogens, hydrogen, hydrogen chloride, and methyl iodide (Scheme 1), giving compounds analogous to those obtained by starting from **1** (see Experimental Section).

Complex **1** exhibits as basic centers either the iridium(I) or both nitrogen pyridine atoms. Following the reaction course by conductivity measurements and ^1H NMR spectra in $CDCl_3$ solution, we established that the addition of HCl to **1** initially occurs to nitrogen atoms to give the cationic species $[Ir(CO)(Ph_2PPyH)_2Cl][Cl]_2$ and, subsequently, to the iridium(I) center, affording the oxidative-addition product $[Ir(CO)H(Ph_2PPyH)_2Cl_2][Cl]_2$ (**6**). IR, as Nujol mull, and ^1H and $^{31}P\{^1H\}$ NMR, in $CDCl_3$ solution, support for **6** a structure with the hydride *trans* to a chloride ligand and the phosphorus atoms *trans* to one another.

With the aim of accessing binuclear complexes in which two metal atoms are surrounded by the binucleating ligands Ph_2PPy, we examined the reactions of **1** with palladium(II), $HgCl_2$, $[Cu(NCCH_3)_4]^+$, and $TlPF_6$ substrates.

The $Ir^{II}-Pd^{I}$ species $[IrPd(CO)Cl_3(\mu\text{-}Ph_2PPy)_2]$ (**8**) was obtained, nearly quantitatively, by adding a benzene solution of $[Pd(PhCN)_2Cl_2]$ to a solution of **1** in the same solvent (molar ratio 1:1). Compound **8** was characterized by analytical, IR, and NMR spectroscopic data and by a single-crystal X-ray diffraction study. The IR spectrum as a Nujol mull shows ν(CO) at 2016 cm^{-1}, indicating the occurrence of an oxidative-addition process at the iridium(I) center. In the ^1H NMR spectrum in $CDCl_3$ solution, the resonances of the 6-hydrogen atoms of the pyridine rings are shifted to higher frequency, as is usually observed when the pyridine nitrogen atom is coordinated.[12] The $^{31}P\{^1H\}$ NMR spectrum in $CDCl_3$ solution shows a single resonance at δ −12.80 ppm, indicating a head-to-head configuration of the Ph_2PPy bridging ligands.

The reaction of **1** with $HgCl_2$, in a 1:1 molar ratio in benzene, afforded as final product the binuclear complex $[Ir(CO)Cl(\mu\text{-}Ph_2PPy)_2HgCl]$ (**9**) as a white solid. Compound **9** is not conducting in benzene solution; it was characterized by elemental analysis and spectroscopic IR and NMR data. All attempts to obtain crystals of **9** suitable for an X-ray diffraction analysis failed. The IR spectrum (ν(CO) 2026 cm^{-1}, Nujol mull) indicates that the reaction occurred with oxidative addition to the iridium(I) center. The $^{31}P\{^1H\}$ NMR spectrum in $CDCl_3$ solution shows a single resonance at δ 16.83 ppm, while, significantly, the ^1H NMR exhibits a shift of 0.5 ppm (δ 9.27 ppm) in the resonances due to the H-6 atoms of the pyridine rings with respect to **1**. IR and NMR data support for **9** a structure with the Ph_2PPy ligands bridging the Ir and Hg metals in a head-to-head configuration. The iridium center assumes an octahedral geometry owing to the coordination of CO and of two chloride ligands and the formation of the Ir−Hg bond.

The reaction of **1** with $HgCl_2$, in benzene, in a 1:2 molar ratio afforded the reaction product $[Ir(CO)(Cl)_2(HgCl_2)(\mu\text{-}Ph_2PPy)_2HgCl]$ (**10**). It was structurally similar to **9** and contained one $HgCl_2$ molecule interacting with the chloride bonded to iridium and *trans* to the Ir−Hg bond (Figure 2). The spectroscopic IR and NMR data of **10** are almost identical with those of **9**; however, the full characterization of **10** was obtained by an X-ray crystal structure analysis.

The reaction of **1** with $[Cu(NCCH_3)_4]BF_4$ and $TlPF_6$ in benzene in a 1:1 molar ratio afforded, almost quantitatively, orange and red compounds, respectively. Both are conducting in methanol solution ($(1-5) \times 10^{-4}$ M) as 1:1 electrolytes. Analytical and spectroscopic data support their formulation as the ionic compounds $[Ir(CO)Cl(\mu\text{-}Ph_2PPy)_2Cu]BF_4$ (**11**) and $[Ir(CO)Cl(\mu\text{-}Ph_2PPy)_2Tl]PF_6$ (**12**). Compounds **11** and **12** are soluble in chlorinated solvents, acetone, methanol, and, to a minor extent, benzene to give air-sensitive solutions. The $^{31}P\{^1H\}$ NMR spectra of **11** and **12** in $CDCl_3$ solution show singlets at δ 27.44 and δ 23.20 ppm, respectively, and support a structure with head-to-head bridging Ph_2PPy ligands.[12] As expected, in the ^1H NMR spectra in $CDCl_3$ solution, the 6-hydrogen of the pyridine ring is shifted to higher frequency (δ 9.39 and 9.15 ppm, respectively) with respect to **1**.[12]

A comparison of the electronic absorption spectrum of **1** with that of **12** shows evidence of the Ir−Tl bonding (Figure 1). The spectrum of **1** (trace A) is typical of Vaska-like complexes. The changes observed on going from trace A (**1**) to trace B (**12**) reflect the existence of the Ir−Tl bonding. Following the suggestion of Balch *et al.*[15] absorption of **12** at 380 nm (ϵ = 6600 M^{-1} cm^{-1}) is assigned to the Ir−Tl chromophore with the weak feature at 470 nm (ϵ = 420 M^{-1} cm^{-1}) taken as its forbidden counterpart. Complex **12** is luminescent in a frozen dichloromethane solution at 77 K. The emission spectrum (excitation in the 350−450 nm range) shows a intense band peaking at 580 nm (trace C). The luminescence lifetime is 5 ns (±10%). The solution of **12** does not show luminescence at 25 °C.

A compound which can be related to **11** was recently obtained[16] in our laboratory by reacting *trans*-$[Rh(CO)(Ph_2PPyOMe)_2Cl]$ with $[Cu(NCCH_3)_4]BF_4$. The product, characterized by the X-ray crystal structure as $[Rh_2Cu(CO)_2(Ph_2PPyOMe)_2(\mu\text{-}Cl)_2]BF_4$, shows the Cu atom almost linearly coordinated to pyridine nitrogen atoms of Ph_2PPy ligands of two rhodium(I) centers.

Crystal and Molecular Structure of $[Ir(CO)(Cl)_2(\mu\text{-}Ph_2PPy)_2PdCl]$ (8). A view of the molecular structure of **8** with the corresponding atom-labeling scheme is shown in Figure 2; water molecules of crystallization are omitted for clarity. Selected bond distances and angles are given in Table 2. The Ir−Pd distance (2.6135(10) Å) is consistent with the presence of a single

(13) (a) Vaska, L. *Acc. Chem. Res.* **1968**, *1*, 335. (b) Collman, J. P.; Roper, W. R. *Adv. Organomet. Chem.* **1968**, *7*, 54. (c) Deeming, A. J. In *Reaction Mechanisms in Inorganic Chemistry*; Emeleus, H. J., Ed.; Inorg. Chem. Ser. 9; Butterworths: Oxford, U.K., 1972; Chapter 4. (d) Vaska, L.; Di Luzio, J. W. *J. Am. Chem. Soc.* **1962**, *84*, 680.

(14) (a) Kubas, G. J. *Inorg. Chem.* **1979**, *18*, 182. (b) La Placa, S. J.; Ibers, J. A. *Inorg. Chem.* **1966**, *5*, 405.

(15) (a) Balch, A. L.; Neve, F.; Olmstead, M. M. *J. Am. Chem. Soc.* **1991**, *113*, 2995. (b) Balch, A. L.; Neve, F.; Olmstead, M. M. *Inorg. Chem.* **1991**, *30*, 3395. (c) Brady, R.; Flynn, B. R.; Goeffroy, G. L.; Gray, H. B.; Peone, J., Jr.; Vaska, L. *Inorg. Chem.* **1976**, *15*, 1485.

(16) Arena, C. G.; Faraone, F.; Lanfranchi, M.; Rotondo, E.; Tiripicchio, A. *Inorg. Chem.* **1992**, *31*, 4797.

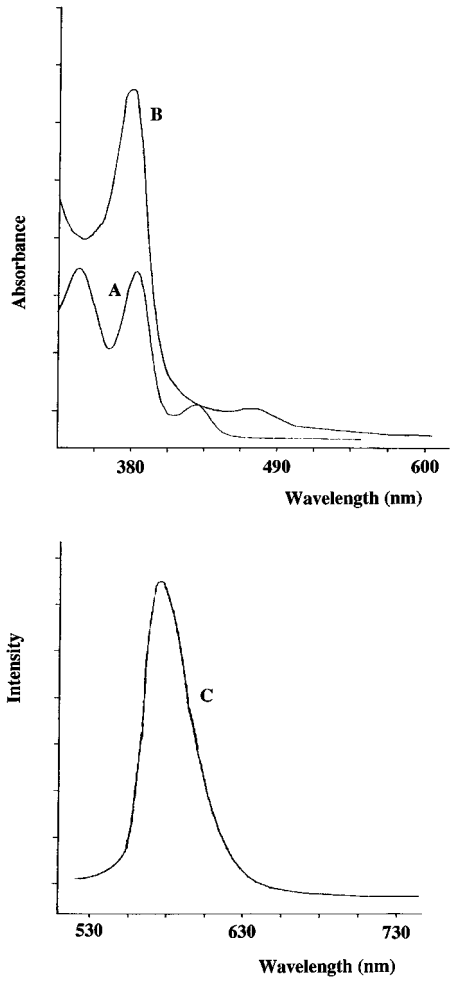

Figure 1. Electronic absorption spectra of (A) [Ir(CO)(Ph_2-PPy)$_2$Cl] (**1**) and (B) [Ir(CO)(Cl)(μ-$Ph_2PPy)_2$Tl][PF_6] (**12**) in dichloromethane solution at 25 °C. Emission spectrum (excitation in the 350−450 nm range) of (C) [Ir(CO)(Cl)(μ-$Ph_2PPy)_2$Tl][PF_6] (**12**) in a frozen dichloromethane solution at 77 K.

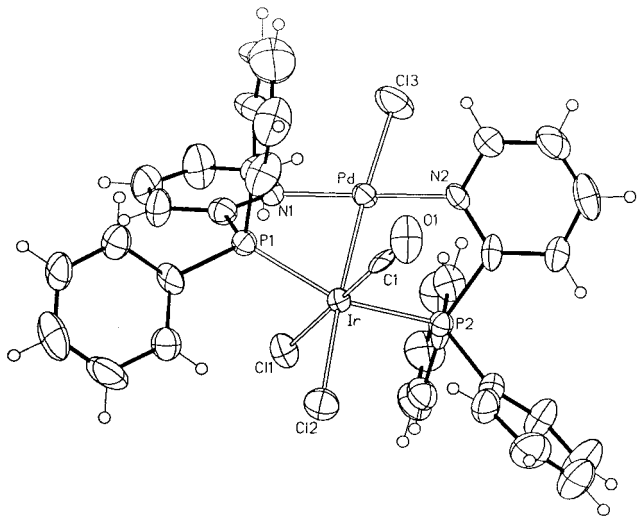

Figure 2. ORTEP view of the structure of **8** with the atomic numbering scheme.

intermetallic bond. This distance is shorter than the corresponding one reported for the only X-ray-characterized IrPd heterobimetallic complex [PdIr(CO)Cl(μ-dpmp)$_2$][PF_6]$_2$ (dpmp = bis((diphenylphosphino)methyl)-phenylphosphine) (Ir−Pd = 2.694(2) Å):[17] and is comparable with the value of 2.594(1) Å reported for the complex RhPd(μ-$Ph_2PPy)_2$(CO)Cl_3,[18] analogous to **8**, where nevertheless the bridging ligands are arranged head-to-tail.

Table 2. Selected Bond Lengths (Å) and Angles (deg) of 8

Ir−C(1)	2.01(2)	Ir−P(1)	2.334(3)
Ir−P(2)	2.334(3)	Ir−Cl(1)	2.391(3)
Ir−Cl(2)	2.508(3)	Ir−Pd	2.614(1)
C(1)−O(1)	0.94(2)	Pd−N(2)	2.034(9)
Pd−N(1)	2.04(1)	Pd−Cl(3)	2.389(4)
P(1)−C(7)	1.81(1)	P(1)−C(6)	1.82(1)
P(1)−C(13)	1.87(2)	P(2)−C(30)	1.80(1)
P(2)−C(24)	1.82(1)	P(2)−C(23)	1.84(1)
C(1)−Ir−P(1)	92.4(4)	C(1)−Ir−P(2)	91.3(4)
P(1)−Ir−P(2)	157.2(1)	C(1)−Ir−Cl(1)	176.5(4)
P(1)−Ir−Cl(1)	86.9(1)	P(2)−Ir−Cl(1)	90.8(1)
C(1)−Ir−Cl(2)	91.1(4)	P(1)−Ir−Cl(2)	105.2(1)
P(2)−Ir−Cl(2)	97.3(1)	Cl(1)−Ir−Cl(2)	85.8(1)
C(1)−Ir−Pd	89.8(4)	P(1)−Ir−Pd	78.97(8)
P(2)−Ir−Pd	78.53(8)	Cl(1)−Ir−Pd	93.44(9)
Cl(2)−Ir−Pd	175.71(9)	O(1)−C(1)−Ir	172(2)
N(2)−Pd−N(1)	178.7(4)	N(2)−Pd−Cl(3)	89.0(3)
N(1)−Pd−Cl(3)	91.4(3)	N(2)−Pd−Ir	88.8(3)
N(1)−Pd−Ir	90.9(3)	Cl(3)−Pd−Ir	176.2(1)

The coordination around the iridium atom is octahedral, albeit strongly distorted. The P(2)−Ir−P(1) bond angle of 157.18(11)° has a significant deviation from linearity. This deviation is due to the head-to-head coordination of the Ph_2PPy bridging ligands. In 16 bimetallic compounds containing Ph_2PPy ligands coordinated head-to-tail, the P−M−N bond angles range from 169.39° (refcod = KUNTOK) to 179.48° (DUSGIH) (Cambridge Structural Database).[19] As expected, the nonbonded P···N separations (P(1)···N(1) = 2.66(1) Å and P(2)···N(2) = 2.69(2) Å) are longer than the metal−metal separation. Torsion angles P(1)−Ir−Pd−N(1) and P(2)−Ir−Pd−N(2) are −40.0(3) and −45.1(3)°, respectively, indicating a great strain in the Ph_2PPy ligand.

The equatorial bond angles around the iridium atom are C(1)−Ir−Cl(2) = 91.1(4)°, Cl(1)−Ir−Cl(2) = 85.75(12)°, C(1)−Ir−Pd = 89.8(4)°, and Cl(1)−Ir−Pd = 93.44(9)°, and their sum is 360.0(7)°. The palladium atom is in a nearly square-planar configuration; the least-square-planes calculated for the four binding atoms (Ir, N(1), N(2), and Cl(3)) shows no deviation greater than 0.09(1) Å; the Pd atom is 0.060(1) Å out from this plane. The palladium coordination plane makes an interplanar angle of 43.6(1)° with the equatorial iridium coodination plane.

Most of the bond lengths fall within the ranges usually found. However, the unusual Ir−Cl(2) and Pd−Cl(3) lengths can be attributed to the high *trans* influence of the metal−metal (Ir−Pd) bond.

Molecular packing is mainly determined by normal van der Waals interactions and weak hydrogen bonds, involving chlorine atoms and a water molecule of crystallization.

Crystal and Molecular Structure of [Ir(CO)(Cl)$_2$-(HgCl$_2$)(μ-$Ph_2PPy)_2$HgCl] (10). The crystals of **10** are

(17) Balch, A. L.; Catalano, V. J. *Inorg. Chem.* **1992**, *31*, 2569−2575.
(18) Farr, P. P.; Olmstead, M. M.; Balch, A. L. *Inorg. Chem.* **1983**, *22*, 1229.
(19) Allen, F. H.; Davies, J. E.; Galloy, J. J.; Johnson, O.; Kennard, O.; Macrae, C. F.; Mitchell, E. M.; Mitchell, G. F.; Smith, J. M.; Watson, D. G. *J. Chem. Inf. Comput. Sci.* **1991**, *31*, 187.

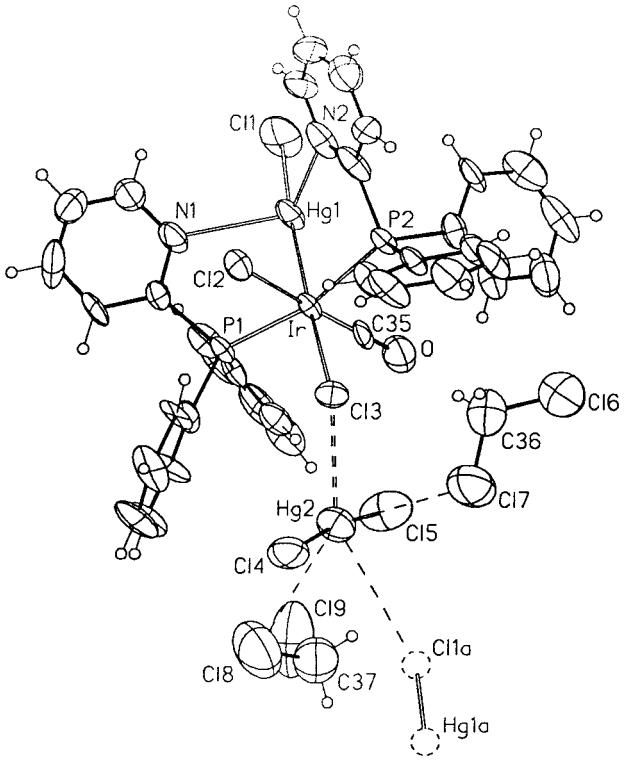

Figure 3. ORTEP view of the structure of **10** with the atomic numbering scheme.

Table 3. Selected Bond Lengths (Å) and Angles (deg) for Complex 10

Hg(1)−Cl(1)	2.394(5)	Hg(1)−N(2)	2.55(2)
Hg(1)−N(1)	2.58(2)	Hg(1)−Ir	2.604(1)
Ir−C(35)	1.73(3)	Ir−P(1)	2.353(4)
Ir−P(2)	2.365(4)	Ir−Cl(2)	2.395(5)
Ir−Cl(3)	2.501(4)	C(35)−O	1.22(3)
Cl(3)−Hg(2)	2.897(4)	Hg(2)−Cl(4)	2.276(6)
Hg(2)−Cl(5)	2.288(6)	P(1)−C(6)	1.81(2)
P(1)−C(12)	1.83(2)	P(1)−C(1)	1.84(2)
P(2)−C(23)	1.81(2)	P(2)−C(29)	1.82(2)
P(2)−C(18)	1.83(2)		
Cl(1)−Hg(1)−N(2)	94.5(4)	Cl(1)−Hg(1)−N(1)	94.5(4)
N(2)−Hg(1)−N(1)	110.3(5)	Cl(1)−Hg(1)−Ir	172.7(2)
N(2)−Hg(1)−Ir	90.1(4)	N(1)−Hg(1)−Ir	89.3(3)
C(35)−Ir−P(1)	96.0(6)	C(35)−Ir−P(2)	92.4(6)
P(1)−Ir−P(2)	166.4(2)	C(35)−Ir−Cl(2)	178.2(6)
P(1)−Ir−Cl(2)	85.8(2)	P(2)−Ir−Cl(2)	85.8(2)
C(35)−Ir−Cl(3)	88.6(6)	P(1)−Ir−Cl(3)	97.0(2)
P(2)−Ir−Cl(3)	93.8(2)	Cl(2)−Ir−Cl(3)	91.1(2)
C(35)−Ir−Hg(1)	89.5(6)	P(1)−Ir−Hg(1)	84.4(1)
P(2)−Ir−Hg(1)	85.0(1)	Cl(2)−Ir−Hg(1)	90.7(1)
Cl(3)−Ir−Hg(1)	177.8(1)	O−C(35)−Ir	177(2)
Ir−Cl(3)−Hg(2)	132.2(2)	Cl(4)−Hg(2)−Cl(5)	171.4(2)
Cl(4)−Hg(2)−Cl(3)	96.6(2)	Cl(5)−Hg(2)−Cl(3)	91.9(2)

formed by cocrystallization of the binuclear complex and two CH_2Cl_2 molecules of solvation. A view of the molecular structure of **10** with the labeling scheme for the non-hydrogen atoms is shown in Figure 3. Selected bond distances and angles are given in Table 3. Two Ph_2PPy groups are bonded head-to-head to the metal centers, both phosphorus atoms being coordinated to iridium. The iridium−mercury bond length of 2.604(1) Å is indicative of a single covalent metal−metal bond; this arises from donation of one electron pair from iridium to mercury. The Ir−Hg bond length is comparable with the value of 2.618 Å found for the complexes $[Cl_2Hg(\mu\text{-}Cl)_2HgIr(CO)Cl(dpm)(\mu\text{-}dpm)AuCl]$ (dpm = diphenylphosphinomethane) and $[Ir(COD)(EpTT)_2HgCl]_2$[20] (EpTT = $C_2H_5N_3$-*p*-$CH_3C_6H_4$) and longer than the value reported for the complex $[IrCl_2(CO)(PPh_3)_2(HgX)]$[21] (X = Cl, Br) (Ir−Hg(Cl) = 2.570(1) Å, Ir−Hg(Br) = 2.578(2) Å). The metal−metal bond distance is shorter than the nonbonded P···N separations (P(1)···N(1) = 2.721 Å and P(2)···N(2) = 2.703 Å); the latter is in the range found for other Ph_2PPy-bridged complexes.[12b] Bond distances and angles for the coordinated Ph_2PPy are nearly alike, as are the P−M−M−N torsion angles P(1)−Ir−Hg−N(1) = 32.2(4)° and P(2)−Ir−Hg−N(2) = −28.9(4)°.

Compound **10** contains three metal centers with different coordination environments. The coordination of the iridium atom can be described as a strongly distorted octahedron. The Ir−P(1) and Ir−P(2) bond distances of 2.353(4) and 2.365(4) Å, respectively, are in the range observed for other iridium−phosphine complexes,[17] while the P(2)−Ir−P(1) bond angle of 166.4(2)° deviates significantly from linearity. The Ir−Cl bond distances are different (Ir−Cl(2) = 2.395(5) Å, Ir−Cl(3) = 2.501(5) Å); the longest one is *trans* to the metal−metal bond.

The atoms coordinated to iridium in the equatorial plane are planar, and the iridium is 0.028(7) Å out of the calculated least-squares plane; the corresponding bond angles range from 88.6(6)° (C(35)−Ir−Cl(3)) to 91.1(2)° (Cl(2)−Ir−Cl(3)), and their sum is 359.9(3)°.

The mercury bonded to the iridium atom shows a very distorted tetrahedral coordination; it is bonded to a chlorine atom (Hg(1)−Cl(1) = 2.394(5) Å) and to two nitrogen atoms (mean Hg(1)−N = 2.565 Å); the Hg−N values are comparable to the value of 2.595(6) Å found in $[FeHg(\mu\text{-}Ph_2PPy)_2(CO)_3(SCN)_2]$.[22] The small N(1)−Hg(1)−Ir (89.3(3)°) and N(2)−Hg(1)−Ir (90.1(4)°) bond angles are both induced by the bridging Ph_2PPy ligands. The N(1)−Hg(1)−N(2) and Ir−Hg(1)−Cl(1) angles are 110.3(5) and 172.7(2)°, respectively; the last value is indicative of severe distortion in the molecule.

A peculiar aspect of the molecular structure of **10** is the presence of a further $HgCl_2$ molecule; the Hg(2)−Cl(4) and Hg(2)−Cl(5) bond distances of 2.276(6) and 2.288(6) Å, respectively, are in good agreement with the corresponding values found for $HgCl_2$.[23] The Cl(4)−Hg−Cl(5) bond angle of 171.4(2)° deviates from linearity, owing to the interaction of Hg(2) with Cl(3) bonded to the iridium atom (Hg(2)−Cl(3) = 2.897(4) Å), so that Hg(2) becomes pseudo-three-coordinate.

The Hg(2) atom has a nonbonding interaction with Cl(1) of a different molecule of **10** (Hg(2)−Cl(1) = 3.561 Å) at x, $y - 1$, z and with chlorine atoms of the two dichloromethane solvent of crystallization molecules. Molecular packing is mainly determined by normal van der Waals interactions and very weak hydrogen bonds involving the chlorine atoms.

Catalysis. Hydroformylation of styrene has been carried out at temperatures of 60 and 80 °C under 60

(20) (a) Van Vliet, P. I.; Kokkes, M.; Van Koten, G.; Vrieze, K. *J. Organomet. Chem.* **1980**, *187*, 413−426. (b) Balch, A. L.; Catalano, V. J. *Inorg. Chem.* **1992**, *31*, 2730−2734.
(21) Brotherton, P. D.; Raston, C. L.; White, A. H.; Wild, S. B. *J. Chem. Soc., Dalton Trans.* **1976**, 1799.
(22) Zhang, Z. Z.; Xi, H. P.; Zhao, W. J.; Jiang, K. Y.; Wang, R. J.; Wang, H. G.; Wu, Y. *J. Organomet. Chem.* **1993**, *454*, 221−228.
(23) Subramanian, V.; Seff, K. *Acta Crystallogr.* **1980**, *B36*, 2132−2135.

Table 4. Hydroformylation of Styrene[a]

entry no.	catalyst	*P* (atm)	*T* (°C)	conversn (%)[b]	hydr[c]	aldehyde[d] branched	aldehyde[d] linear	*B/L*[e]	TOF[f]
1	*trans*-[Ir(PPh_3)$_2$(CO)Cl]	80	80	6.5	7.8	83.0	9.2	90/10	203
2	*trans*-[Ir(PPh_3)$_2$(CO)Cl]	60	80	1.5	33.4	66.2	0.4	99/1	47
3	*trans*-[Ir(PPh_3)$_2$(CO)Cl] + Py (1:1)	60	80	2.6	34.6	65.0	0.4	99/1	81
4	*trans*-[Ir(Ph_2PPy)$_2$(CO)Cl] (**1**)	80	80	45.8	37.8	56.9	5.3	92/8	1431
5	*trans*-[Ir(Ph_2PPy)$_2$(CO)Cl] (**1**)	80	60	9.8	43.2	53.8	3.0	95/5	306
6	*trans*-[Ir(Ph_2PPy)$_2$(CO)Cl] (**1**)	60	80	56.2	46.1	40.1	3.8	91/9	1756
7	*trans*-[Ir(Ph_2PPy)$_2$(CO)Cl] + Ph_2PPy (1:3)	80	80	42.3	41.7	52.3	6.0	90/10	1322
8	[IrCu(μ-Ph_2PPy)$_2$(CO)Cl][BF_4]	80	80	51.1	35.0	58.7	6.3	90/10	1597
9	[IrCu(μ-Ph_2PPy)$_2$(CO)Cl][BF_4]	80	60	31.8	8.2	85.2	6.6	93/7	994
10	[IrCu(**μ**-Ph_2PPy)$_2$(CO)Cl][BF_4]	60	80	64.5	51.8	41.2	7.0	85/15	2016
11	[IrCu(**μ**-Ph_2PPy)$_2$(CO)Cl][PF_6]	80	80	53.5	40.2	53.1	6.7	89/11	1672
12	[IrCu(**μ**-Ph_2PPy)$_2$(CO)Cl][PF_6]	60	80	70.3	55.9	40.2	3.9	91/9	2197

[a] Reaction conditions: solvent benzene (10 mL); $CO/H_2 = 1$; catalyst:styrene = 1:500. [b] Determined by GC analysis. [c] Ethylbenzene. [d] Branched aldehyde 2-phenylpropionaldehyde, linear aldehyde 3-phenylpropionaldehyde. [e] *B/L* = branched/linear. [f] TOF = [(mol of product)/(mol of cat.)(reaction time)] × 100.

and 80 atm of CO and H_2 (1:1), with relevant results being obtained using **1**, **11,** and **12** as catalytic precursors (Table 4). After a typical reaction time of 16 h, the crude reaction mixture was analyzed and the ratio between 2-phenylpropanal, 3-phenylpropanal, ethylbenzene, and unreacted styrene was determined by gas chromatographic analysis and NMR spectroscopy. At first the hydroformylation of styrene was carried out at 80 °C and under 80 atm of CO and H_2 (1:1) using as precatalyst *trans*-[Ir(CO)(PPh_3)$_2$Cl] (entry 1). As expected, the catalytic activity observed was very low, with a styrene conversion of 6.5%. The regioselectivity in the branched aldehyde 2-phenylpropanal was in the ratio 90:10, while the ethylbenzene formed was 7.7%. Significantly, the addition of an excess of free pyridine to the catalytic system based on Vaska's complex does not change significantly the yield of the styrene conversion (entry 3). Operating at 80 °C and under 60 atm lowered the styrene conversion to 1.5%. Comparison of these results with those obtained, under the same experimental conditions, using **1** as catalytic precursor (entry 4) demonstrates that the presence of the pendant pyridine significantly increases the rate of the catalytic process. At 80 °C and under 80 atm of CO and H_2 (1:1) pressure, the styrene conversion increases to 37.6% using **1** as catalytic precursor. Also the regioselectivity increases to a 2-phenylpropanal to 3-phenylpropanal ratio of 92:8. The chemoselectivity of the process was low, the hydrogenated product ethylbenzene being 37.8%. When the reaction pressure is reduced to 60 atm (entry 6), the conversion increases while the regioselectivity remains unchanged. In the rhodium-catalyzed hydroformylation of styrene, by reduction of the CO/H_2 pressure, the conversion decreases because the σ-acyl derivative is formed in minor yield. This occurs also in the hydroformylation with **1**. In fact, the comparison of entries 4 and 6 makes evident that when the pressure is reduced to 60 atm, the yield of aldehydes decreases although the amount of styrene conversion increases. It is noteworthy that the activity of the catalytic system becomes negligible under 80 atm as the temperature is lowered to 60 °C (entry 5). The addition of free Ph_2PPy, in the molar ratio 1:3, to the catalytic system based on **1** does not change significantly the yield of the styrene conversion (entry 7), indicating that dissociation of Ph_2PPy from **1**, under equilibrium conditions, does not occur during the catalytic cycle.

Using complexes **8**−**10** as catalytic precursors at 80 °C and 80 atm of CO/H_2 pressure, we did not observe significant conversion of styrene. Surprisingly, complexes **11** and **12** exhibit catalytic activity with results comparable to those for **1** (entries 8−12) under the same experimental conditions. Analogous to the situation observed with **1**, reducing the reaction pressure to 60 atm (entries 11 and 12), gives an increase in styrene conversion, although the aldehydes were formed to a minor extent.

Discussion

There are in the literature various homo- and heterobinuclear complexes in which d^8 metal atoms are surrounded by two binucleating Ph_2PPy ligand molecules. Surprisingly, to our knowledge,[5] there are no complexes of iridium reported. We prepared the bimetallic complexes **8**−**12** (Scheme 1) using a bridge-assisted method.[24]

An important aspect of the reactions of **1** with [Pd($PhCN$)$_2$Cl$_2$] and $HgCl_2$ is the change in the formal oxidation states of metal centers in the products **8**−**10** with respect to reagents. Very likely, the first step of the reaction of **1** with [Pd($PhCN$)$_2$Cl$_2$] is nucleophilic attack of the Ph_2PPy nitrogen atoms of **1** on the palladium(II) center to give an intermediate Ir^I-Pd^{II} species, namely [(CO)ClIr(μ-Ph_2PPy)$_2$PdCl$_2$]. The oxidative addition of a Pd−Cl bond across the iridium(I) center leads to the binuclear complex **8**. The capability of the bridging short-bite Ph_2PPy ligand to promote intramolecular redox processes was discussed in previous papers.[12a,18,25−27] Differently, the reaction between the basic iridium(I) center of **1** and the Lewis acid $HgCl_2$ very likely occurs through initial formation of [Ir(CO)Cl$_2$(Ph_2PPy)$_2$HgCl]. This gives **9** by subsequent coordination of the pyridine nitrogen atoms to an unsaturated mercury center, in an intramolecular process. The first step of the reaction was verified[13] in the reaction of Vaska's complex with $HgCl_2$.

(24) Roberts, D. A.; Geoffroy, G. In *Comprehensive Organometallic Chemistry*; Wilkinson, G., Stone, F. G. A., Abel, E. W., Eds.; Pergamon: Oxford, U.K., 1982; Chapter 40.
(25) Farr, P. P.; Olmstead, M. M.; Balch, A. L. *J. Am. Chem. Soc.* **1980**, *102*, 6654.
(26) Lo Schiavo, S.; Rotondo, E.; Bruno, G.; Faraone, F. *Organometallics* **1991**, *10*, 1613.
(27) Farr, P. P.; Olmstead, M. M.; Wood, F. E.; Balch, A. L. *J. Am. Chem. Soc.* **1983**, *105*, 792.

Scheme 2[a]

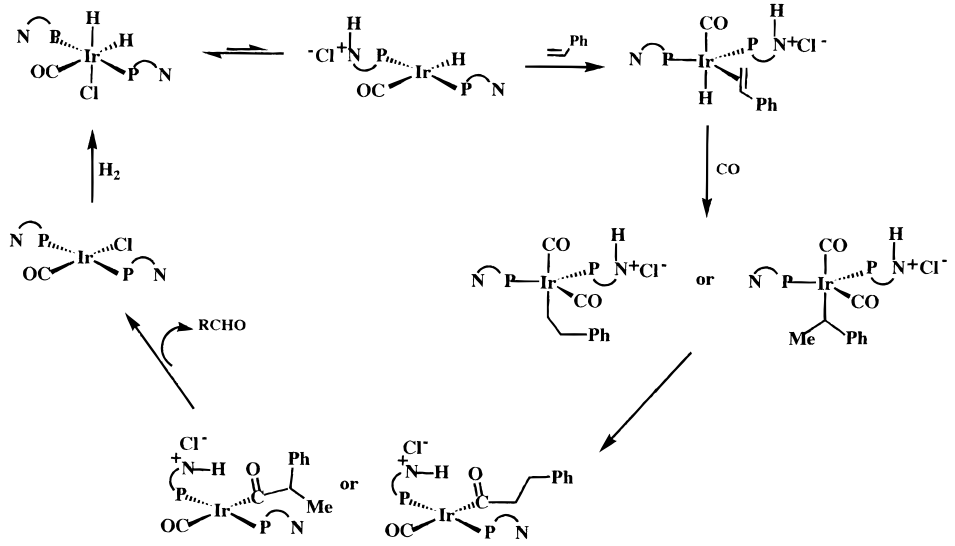

[a] P−N = 2-(diphenylphosphino)pyridine.

The formation of **11** and **12** very likely occurs by nucleophilic attack of the pendant pyridine nitrogen atoms of **1** on the Cu^{I} and Tl^{I} metal center.

The formation of the head-to-head isomer as the only reaction product in the synthesis of bimetallic complexes **8**−**12** assumes particular relevance when we consider that in the analogous compounds of electron-rich metals, such as Rh, Pd, and Pt, the bridged Ph_2PPy ligands assume preferentially a head-to-tail configuration.[25−28] The formation of **8** as the only product in the reaction of **1** with $[Pd(PhCN)_2Cl_2]$ indicates that the head-to-head isomer of **8** is thermodynamically more stable than the head-to-tail one.

Because the formation of the head-to-tail isomer starting from a bis-Ph_2PPy P-bonded species involves the breaking of one metal−phosphorus bond, the strength of the Ir−P bond is a factor determining the structure of the isomers. The formation of the head-to-head isomers starting from **1** is in line with the strength of the metal−phosphorus bond, which is for the third-row transition metals more than that of the second row.

The results of this study clearly show that the coordination of Ph_2PPy ligands to an iridium(I) center causes a pronounced effect on the catalytic activity of the precatalyst **1** in the hydroformylation of styrene. In fact, as expected, under the same experimental conditions of **1**, Vaska's complex displays negligible catalytic activity. These results indicate that the drastic change in the activity of the two catalytic systems can only be due to the presence of basic uncoordinated pyridine nitrogen atoms in the pendant Ph_2PPy ligands of **1**. Scheme 2 represents the fundamental steps of the proposed catalytic cycle. Very likely the protonation, under equilibrium conditions, of the uncoordinated nitrogen atom assists the reductive elimination of HCl from the iridium(III) species $[Ir(CO)(H)_2(Ph_2PPy)_2Cl]$, formed in the first step of the process by addition of H_2 to **1**. The cationic four-coordinate iridium(I) intermediate $[Ir(CO)(H)(Ph_2PPyH)(Ph_2PPy)]Cl$ was not detected by NMR spectroscopy of the reaction mixture, described herein, of **1** with H_2 because the equilibrium between the dihydride and the cationic species results in a complete shift toward the iridium(III) species. In the catalytic cycle the cationic four-coordinate iridium(I) $[Ir(CO)(H)(Ph_2PPyH)(Ph_2PPy)]^+$ intermediate or the corresponding dicarbonyl five-coordinate species can react with the styrene, affording the five-coordinate species $[Ir(CO)(H)(styrene)(Ph_2PPyH)(Ph_2PPy)]^+$; this, in turn, inserts the coordinated olefin into the Ir−H bond to give the corresponding σ-alkyl derivative; the resulting vacant coordination site can be occupied by carbon monoxide. Subsequently, the migratory insertion of CO into the Ir−C σ-bond will give the iridium−acyl species (branched or linear). The final step, resulting in the aldehydes 3-phenylpropanal and 2-phenylpropanal, involves protonolysis, by the N-protonated P-monodentate ligands Ph_2PPyH^+, of the iridium(I)−acyl species and coordination of chloride to the metal center to give **1**. The protonolysis of the acyl group does not occur under equilibrium conditions and indicates that protonation of the pyridine nitrogen atom in the pendant Ph_2PPy was not stoichiometric. In accordance, the addition of free pyridine to Vaska's complex (entry 3) does not significantly increase the styrene conversion under the catalytic conditions.

As for rhodium-catalyzed hydroformylation,[29,30] the regioselectivity of the process is determined in the step that converts $[Ir(CO)(H)(styrene)(Ph_2PPyH)(Ph_2PPy)]^+$ into a branched or linear four-coordinate σ-alkyl intermediate. The Ph_2PPyH^+ group, as the short-bite bifunctional ligand Ph_2PPy, is rigid. In the intermediate $[Ir(CO)_2(acyl)(Ph_2PPyH)(Ph_2PPy)]^+$ the Ir−P bond places the protonated pyridine nitrogen atom in close proximity to the Ir−C bond. Under these conditions the protonolysis of the coordinated acyl group is very easily achieved. Such an effect can be called the "symphoria

(28) (a) Maisonnat, A.; Farr, J. P.; Balch, A. L. *Inorg. Chim. Acta* **1981**, *53*, L217. (b) Farr, J. P., Wood, F. E.; Balch, A. L. *Inorg. Chem.* **1983**, *22*, 3387.

(29) (a) Casey, C. P.; Whiteker, G. T.; Melville, M. G.; Petrovich, L. M.; Gavney, J. A., Jr.; Powell, D. R. *J. Am. Chem. Soc.* **1992**, *114*, 5535. (b) Gladiali, S.; Bayon, J. C.; Claver, C. *Tetrahedron: Asymmetry* **1995**, *6*, 1453.

(30) Brown, J. M.; Kent, A. G. *J. Chem. Soc., Perkin Trans.* **1987**, *2*, 1597.

effect",[31] as the acyl group and the proton of Ph_2PPyH^+ are in the right position to interact.

A noteworthy aspect of the hydroformylation of styrene using **1** as catalyst precursor is the low chemoselectivity of the process, with yields of the hydrogenated product ethylbenzene ranging between 38 and 46%. In the catalytic cycle ethylbenzene can be formed through protonolysis of the linear or branched σ-alkyl derivative intermediates by means of the P-monodentate ligand Ph_2PPyH^+. This step can be operative because the Ir−P bond is efficient enough to hold the proton in proximity of the Ir−C(alkyl) bond before CO insertion to give the corresponding acyl derivative. The ratio of ethylbenzene to aldehydes is dependent on the relative rate of the CO insertion and protonolysis steps. In principle, protonolysis by PPh_2PyH^+ can occur either on the Ir−acyl or on the Ir−alkyl bonds. Thus, the protonolysis steps determine the chemoselectivity and the overall reaction rate of the catalytic cycle.

In Scheme 2 the dissociation under equilibrium conditions of one Ph_2PPy ligand from **1** or from the dihydride species was not considered. However, these steps are considered to occur in the hydroformylation of olefins by Wilkinson's catalyst. We observed (entry 7) that the presence of free Ph_2PPy does not modify the conversion of styrene.

Surprisingly, using complexes **11** and **12** as precursor catalysts, we observed catalytic activity which compares very well to that of **1**.

(31) Morrison, R. T.; Boyd, R. N. *Organic Chemistry*; Prentice-Hall: Englewood Cliffs, NJ, 1992; Chapter 29.

We proved that, under the catalytic experimental conditions, the Cu−N and Tl−N bonds are broken to give **1**. The occurrence of Cu−N and Tl−N bond ruptures in **11** and **12** is supported by the fact that, in benzene solution at 60 °C and under 60 atm of CO/H_2 (1:1), these complexes afford as major product, together with an uncharacterized compound, the five-coordinated species $[Ir(CO)_2H(Ph_2PPyH)(Ph_2PPy)]^+$ as yellow solid. Spectroscopic IR and NMR data indicate for this compound a structure with the hydride and CO in axial positions. The compound shows in the IR spectrum two ν(CO) bands at 2053 and 2085 cm^{-1}. It exhibits in the $^{31}P\{^1H\}$ NMR ($CDCl_3$ solution) a singlet at δ 9.30 ppm and, in the hydride region of the ^1H NMR ($CDCl_3$) spectrum, a triplet at δ −10.34 ($^2J_{HP}$ 15.6 Hz). These data support the proposed structure if we consider that the protonation of the pyridine nitrogen atom of pendant Ph_2PPy does not modify the phosphorus chemical shift and the $^2J_{HP}$ value of the ligand.

Acknowledgment. Financial support from MURST and the Italian CNR is gratefully acknowledged.

Supporting Information Available: Tables SI−SIX, giving fractional atomic coordinates and *U* values for the nonhydrogen atoms, hydrogen atom coordinates, anisotropic thermal parameters, and complete bond lengths and bond angles for compounds **8** and **10** and a crystal-packing diagram for **10** (18 pages). Ordering information is given on any current masthead page.

OM970145N